T2

:

[1]

. . . . . . [2] , [3]

: T2

(Magnetic Resonance Urography; MRU)

.

: MRU (Percutane- ous
nephrostomy, PCN) (Antegrade pyelography, AGP)
25 . Half- Fourier acquisition single- shot turbo spin- echo
(HASTE) T2 MRU 3- Dimensional fast imaging with steady state
precession (3- D FISP) T1 MRU .
MRU AGP

, , AGP
HASTE 3- D FISP .
: 3- D FISP MRU T2 MRU
($p= 0.002$). AGP HASTE
T2 MRU 19 (76%), 3- D FISP MRU 21
(84%) . AGP HASTE
18 (72%), 3- D FISP 22 (88%) .
3- D FISP MRU T2 MRU
($p= 0.003$).
: T2 MRU T1 MRU
,

.

(Antegrade Pyelography, AGP)

(Intravenous Urography, IVU) . ,
(1). , (invasive technique)

, IVU

(4).

(2- 3).
(Retrograde Pyelography, RGP) , T2
T2 (MR
Urography, MRU)

[1]
[2] ,
[3]

2001 6 18 2001 10 10 . (5- 8). , T2

: T2

AGP, RGP, , CT, MRU), (2),
(4) (Table 1).

MRU 6

. MR

(Contrast enhanced excretory MR urography,
CEMRU)
(9- 11).
PCN AGP
T2 MRU CEMRU MRU
PCN

1.5 Tesla Unit (Magnetom Vision unit, Siemens AG, Erlagen,
Germany) ,
(phase array coil) . MR
T2 HASTE TR 11.9 ms, TE 95 ms,
(flip angle) 150°, acquisition 1, (field of
view) 245× 280 350× 350 , (matrix
size) 115× 256 4 mm
13
15 (source images)
(Maximum intensity projection, MIP)

25 8
2 (nephrectomy)
. 27 82 (
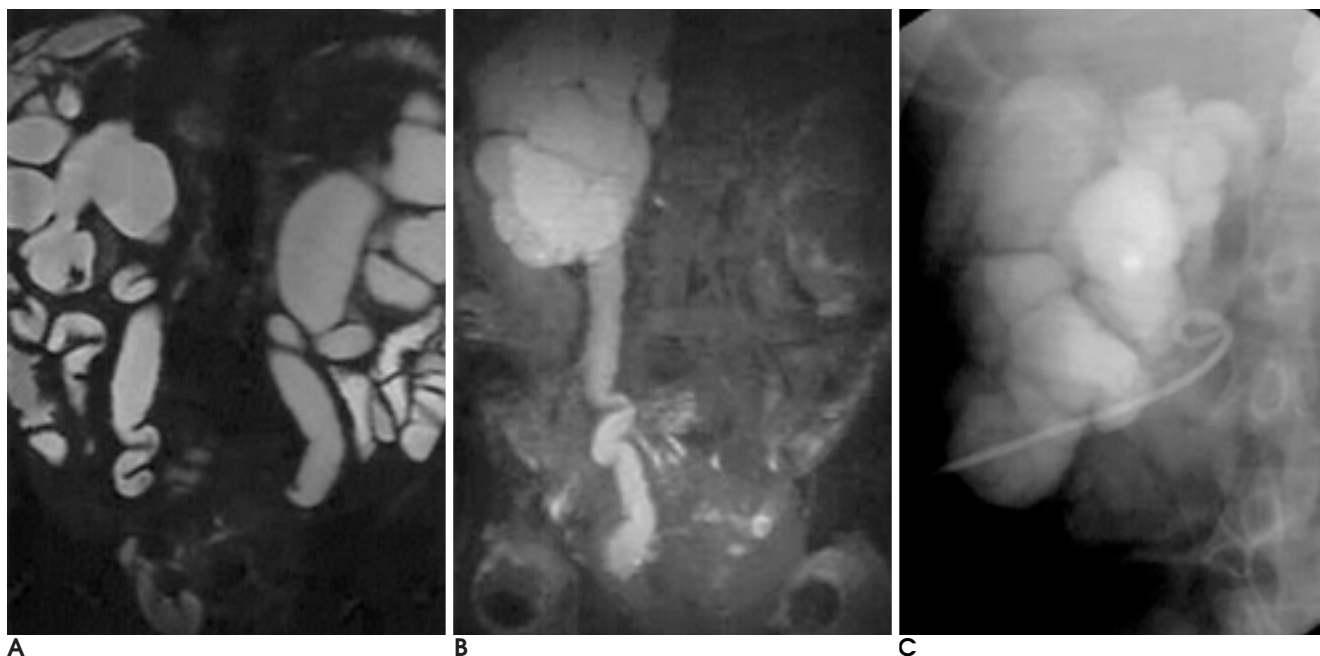55.8) 14:11 . ,
, IVU
, PCN
.
, , , (IVU,

Table 1. Final Clinical Diagnoses in 25 Patients

Diagnosis	No. of patients
Ureter stone	4
Anomaly of the urinary tract	1
Bladder outlet obstruction	1
Psoas muscle abscess	1
Benign stricture of urinary tract	13
Bladder cancer involving ureter	3
Transitional cell carcinoma	2

A   **B**   **C**

Fig. 1. A-57-year-old man with bladder cancer.
A. MIP image of HASTE MRU shows both hydronephrosis due to malignant obstruction of both ureters by invasion of bladder cancer at ureterovesical junction.
B. MIP image of CEMRU shows contrast excretion into right pelvocalyceal system but doesn' t show excretion into left one, which suggests that right renal function is better than that of left kidney. Therefore, right kidney was selected for the site of percutaneous nephrostomy.
C. Antegrade pyelography (AGP) obtained after PCN shows severe hydronephrosis of right kidney.

19

(delineation)

. CEMRU (Lasix; Hoechst, AGP . AGP
Frankfurt/Main, Germany) 20 mg (intravenous injec- 3 , AGP
tion) , 30 1 (paramagnetic sub- 2 , AGP
stance) kg 0.1 mmol 1 Wilcoxon
. CEMRU (3- signed rank test .
D gradient-echo sequences) TR 5 ms, TE 2 ms, , , AGP T2
40°, 115× 256, 285× 380, slice 2 MRU CEMRU MR
mm 3 , 5 , 20 30 , (type)
.

24
. CEMRU MIP ,
. .
MRU 1-3 PCN , AGP (smooth tapering)
PCN 10-50 cc
(Ioxitalamate, Telebrix) (abrupt cutting), (caliber
change),

. T2 MRU CEMRU AGP
T2 MRU T1 CEMRU ,
PCN AGP AGP
. 4 , AGP
3 ,
(delineation) , , AGP 2 ,
2 AGP
. HASTE MRU 3D-FISP 1 ,
CEMRU Wilcoxon signed rank test .

A

B
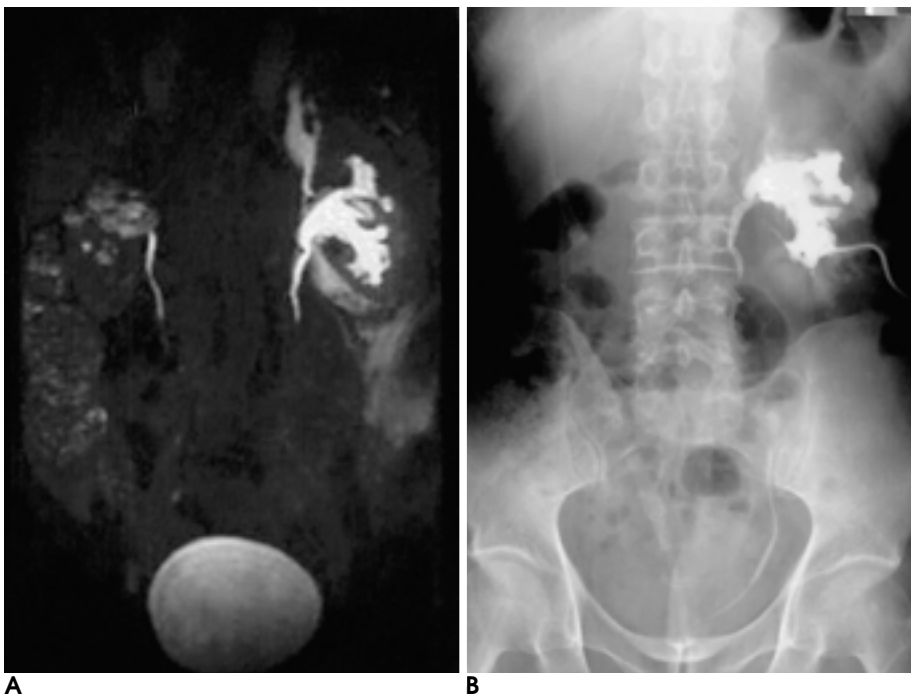
Fig. 2. A-63-year-old man with benign stricture of left ureter and extravasation of contrast material due to forniceal rupture.
A. MIP image of CEMRU reveals complete obstruction of left proximal ureter. Extravasation of contrast material into perirenal space is noted.
B. AGP shows incomplete obstruction of proximal ureter with the contrast passage into the bladder.

: T2

(Fig. 3),

1 AGP

T2 MRU
8 T2 MRU (signal void)
CEMRU MRU AGP
,
(non- enhanced helical) CT
PCN (Fig. 1). 1 .
CEMRU 5 MRU 5 AGP 4
T2 MRU (Fig. 4).
(*p*= 0.002) (Table 2). T2
MRU 19 (76%) , CEMRU 21
(84%) AGP .
MRU AGP T2
. AGP 20 T2 HASTE
5 , T2 MRU rapid acquisition with relaxation enhancement (RARE)
18 (72%) CEMRU 22 (88%) , MRU
. 1 T2 MRU
, CEMRU
(spontaneous forniceal rupture)

, AGP

(Fig.
2). CEMRU
T2 MRU
(*p*= 0.003) (Table 2).
4 MRU AGP 2
. 1 AGP
MRU

Table 2. Comparison of T2-weighted MRU with CEMRU in Terms of the Depiction of Pelvocalyceal System and Causes of Obstructions

	T2-WI MRU*	CEMRU*	P-value[†]
Depiction of pelvocalyceal system	1.56± 0.77	1.96± 0.79	0.002
Causes of obstructions	2.16± 0.89	2.52± 0.82	0.003

* : T2-weighted MRU using HASTE sequence and T1-weighed contrast enhanced MRU using 3-D FISP sequence
[†] : significant difference with *p* < .05
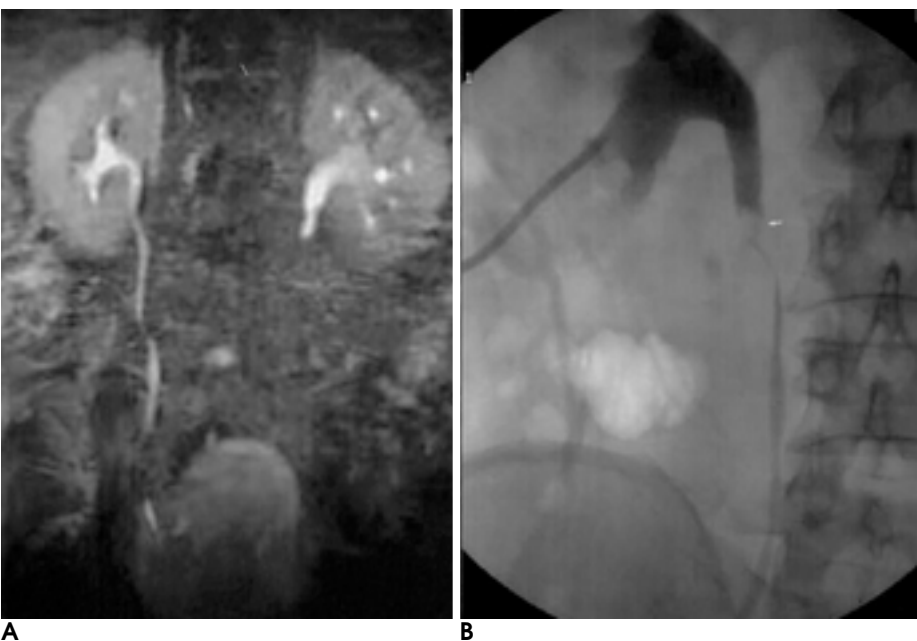
Fig. 3. A-65-year-old man with left ureteral stone.
A. MIP image of CEMRU shows stricture of left proximal ureter. However, the cause of obstruction is not definitely seen.
B. AGP shows a round filling defect (arrow) at the proximal ureter clearly, which was proved a stone.

A B
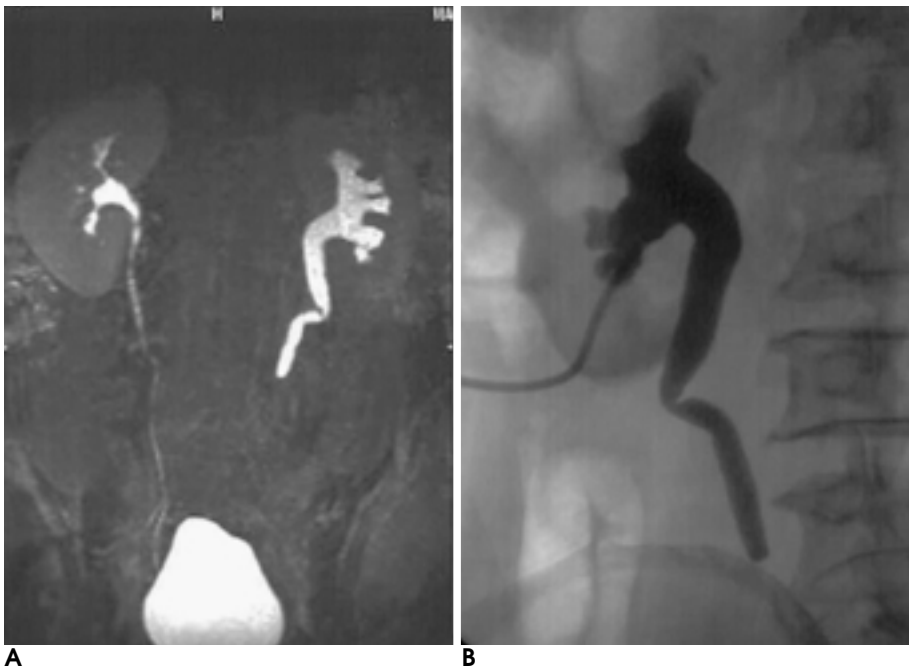
Fig. 4. A-67-year-old man with transitional cell carcinoma of left ureter.
A. MIP image of CEMRU demonstrates an abrupt ending of contrast filled ureteral column at the proximal ureter.
B. AGP demonstrates complete obstruction of the left ureter with abrupt cutting sign.

(2, 8, 12- 14).   T2   MRU   IVU
                                                                                                           ,
                  ,   T1   MRU
                                                            (9,
11).   MRU
          RGP   AGP   (17).
                                                                          T2   MRU
          ,

                                                                          PCN
                  (12, 15).   , T2   MRU   T1   PCN
    CEMRU   AGP   . CEMRU
                                       .   (grade II   )
T2   MRU   (grade III   5- 20   .
)   ,   T2   MRU   (ampu-
          (excretion)   CEMRU   tation)   ,
    ,   .
                                                 CEMRU   T2   MRU
      ,   .   .
      ,   T2   MRU   T1
                                                 MRU

    (superimposition)   CEMRU   3
                  (13, 14, 16).   (whole length)
T2   MRU   CEMRU
        ,
                                    .   (9, 11).
                                                 AGP   MRU   MIP
          3- D FISP CEMRU

53

: T2

,

.

. , MRU AGP RGP

2

, 5 mm

1 mm . ,

(7, 9, 12, 16).

6

· ,

1

.

, CEMRU T2 MRU

, MRU

2 AGP

. T2 MRU

, CEMRU

, (single kid-

ney)

PCN .

, MRU AGP

RGP

.

1. Cronan JJ. Contemporary concepts in imaging urinary tract ob-struction. *Radiol Clin North Am* 1991;29:527-542

2. Regan F, Bohlman ME, Khazan R, et al. MR urography using HASTE imaging in the assessment of ureteric obstruction. *AJR Am J Roentgenol* 1996;167:1115-1120

3. Berns AS. Nephrotoxicity of contrast media. *Kidney Int* 1989;36: 730-740

4. Schubert RA, Gockeritz S, Mentzel HJ, et al. Imaging in ureteral complications of renal transplantatic value of static fluid MR urog-raphy. *Eur Radiol* 2000;10:1152-1157

5. Rothpearl A, Frager D, Subramanian A, et al. MR urography: Technique and Application. *Radiology* 1995;194:125-130

6. , , . . 1997;37:483-488

7. O' Malley ME, Soto JA, Yucel EK, Hussain S. MR urography: Evaluation of a three-dimensional fast spin-echo technique in pa-tients with hydronephrosis. *AJR Am J Roentgenol* 1997;168:387-392

8. Aerts P, Van Hoe L, Bosmans H, et al. Breath-hold MR urography using HASTE technique. *AJR Am J Roentgenol* 1996:543-545

9. Nolte-Ernsting CC, Bucker A, Adem GB, et al. Gadolinium-en-hanced excretory MR urography after low-dose diuretic injection: Comparison with Conventional Excretory urography. *Radiology* 1998;209:147-157

10. Rofsky NM, Weinreb JC, Bosniak MA, et al. Renal lesion charac-terization with gadolinium-enhanced MR imaging: Efficacy and safety in patients with renal insufficiency. *Radiology* 1991;180:85-89

11. Nolte-Ernsting CC, Tacke J, Adem GB, et al. Diuretic-enhanced gadolinium excretory MR urography: Comparison of conventional gradient-echo sequences and echo-planar imaging. *Eur Radiol* 2001;11:18-27

12. Roy C, Saussine C, John C, et al. Evaluation of RARE-MR urogra-phy in the assessment of ureterohydronephrosis. *J Comput Assist Tomogr* 1994;18:601-608

13. Tang Y, Yamashita Y, Namimoto T, et al. The value of MR urogra-phy that uses HASTE sequence to reveal urinary tract disorders. *AJR Am J Roentgenol* 1996;167:1497-1502

14. Balci NC, Mueller-Lisse UG, Holzknecht N, et al. Breath-hold MR urography: Comparison between HASTE and RARE in healthy volunteers. *Eur Radiol* 1998;8:925-932

15. Gaeta B, Blandino A, Scribano E, et al. Diagnostic pitfalls of breath-hold MR urography in obstructive Urography. *J Comput Assist Tomogr* 1999;23:891-897

16. Nolte-Ernsting CC, Adam GB, Gunther RW. MR urography: Examination techniques and clinical applications. *Eur Radiol* 2001; 11:355-372

17. Knopp MV, Dorsam J, Oesingmann N, et al. Functional MR urog-raphy in patients with renal transplants. *Radiology* 1997;37:233-238

The Usefulness of T2-weighted MR Urography and Contrast Enhanced MR Urography in the Evaluation of Obstructive Uropathy:
Comparisonal Study with Antegrade Pyelography[1]

Chang-Hoon Oh, M.D., Jeong-Min Lee, M.D., Kong-Yong Jin, M.D., Gyung-Ho Chung, M.D.,
Seung-Il Cho, M.D., Sang-Hun Lee, M.D., Gyung-Jae Oh, M.D.[2], Young-Kon Kim, M.D.[3]

[1]Department of Radiology, Chonbuk National University Hospital
[2]Department of Preventive Medicine and Public Health, Chonbuk National University, School of Medicine
[3]Department of Urology, Chonbuk National University Hospital

Purpose: To compare the efficacy of contrast-enhanced and T2-weighted magnetic resonance urography (MRU) for the depiction of obstruction and evaluation of the causes of obstructive uropathy with that of antegrade pyelography.

Materials and Methods: Twenty-five patients with obstructive uropathy who underwent percutaneous nephrostomy (PCN) and antegrade pyelography (AGP) were included in the study. We performed MR urography, comprising half-Fourier acquisition single-shot turbo spin-echo (HASTE) T2-weighted imaging and 3-D fast imaging with steady state precession (3-D FISP) T1-weighted imaging after gadolinium enhancement and compared the quality of the images of both the HASTE and 3-D FISP MRU techniques in terms of their depiction of the dilated pelvocalyceal system, and the level, type, and causes of obstruction.

Results: In terms of anatomical depiction of the pelvocalyceal system ($p=0.002$) and the causes of obstruction ($p=0.003$), T1-weighted MRU using 3D-FISP was significantly better than T2-weighted MRU using the HASTE sequence. Regarding level of obstruction, T2-weighted MRU using the HASTE sequence and contrast-enhanced T1-weighted MRU using 3D-FISP showed an accuracy of 76% (19/25) and 84% (21/25), respectively. In terms of type of obstruction, the accuracy of T2-weighted MRU and T1-weighted CEMRU was 72%(18/25) and 88% (22/25), respectively.

Conclusion: T2-weighted MRU and T1-weighted CEMRU provided both anatomical information and that relating to impaired renal function. The two modelities played a complementary role and their use could decrease the unnecessary use of invasive diagnostic examination for the evaluation of obstructive uropathy.

Index words : Magnetic resonance (MR), technology
Ureter, stenosis or obstruction

Address reprint requests to : Jeong Min Lee, M.D., Department of Radiology, Chonbuk National University Hospital,
Keumam-Dong, 634-18, Deokjin Gu, Chonju Shi, Chonbuk 561-712, South Korea.
Tel. 82-63-250-1176   Fax. 82-63-272-0481